NUCLEAR INSTRUMENTS AND METHODS 105 (1972) 269–275; © NORTH-HOLLAND PUBLISHING CO.

ION BOMBARDMENT INDUCED PHOTON AND SECONDARY ELECTRON EMISSION*

JACQUES G. MARTEL† and N. THOMAS OLSON+

Department of Nuclear Engineering, Massachusetts Institute of Technology, Cambridge, Massachusetts, U.S.A.

Received 29 May 1972

Results of an experimental investigation of photon and secondary electron emissions produced during inelastic collisions between energetic ions and lattice atoms are reported. Cs and Na ions, accelerated to energies of 1 to 20 keV, were used to bombard Al, Au, Cu, Cr, Fe, Ge and Si targets. Alkali metal ions were selected since they have no potential secondary electron emission and direct comparisons between photon and electron emission were possible.

The photon emission observed was that of the line spectra of neutral atoms and no continuous spectra, or plasma oscillation emission, was observed. The intensity of photon emission was linear with the ion beam current density up to 10 μA/cm^2 for cesium and 1 μA/cm^2 for sodium ion bombardment. Above these current densities a saturation, which is not explained, occured. The photon emission intensity increased with ion energy up to approximately 10 keV where a saturation occurred. Target self-absorption of the emitted photons accounts for this saturation, however.

The dependence of the photon emission and the secondary electron emission upon experimental parameters was similar, but not identical. Both emissions originate in inelastic collisions although their means of escape from the target affects their dependence upon experimental parameters.

1. Introduction

When energetic atoms, either neutral or ionized, strike a solid target a number of complex phenomena take place simultaneously. The different means of energy dissipation have been reasonably well classified, although the actual energy exchange mechanisms remain, in many cases, unexplained. A variety of interaction potentials are used to cover the energy range from 10^6 eV to zero and a mass range which is the combination of any two elements. In the low energy limit, the ion does not have enough energy to penetrate the atomic cloud or to transfer significant energy (i.e., energy comparable to the ionization energy) to free electrons. In this energy range, the only energy loss mechanism usually considered is the elastic transfer to lattice atoms.

Although this is a reasonable approximation to make, it is not an accurate description of low energy ion–atom collisions. Inelastic collisions do occur in which electrons are excited or ejected and the struck atom is left in an excited or ionized state. During the collision, the electron clouds of the two colliding particles overlap resulting in a reorganization of their electron states. Energy of the incident particle is given up as kinetic energy to the struck atom, but it is also possible that both electron systems are left in excited states.

The excited electron clouds of the struck atom or the incident ion will return to the ground state by either radiationless (electron) or radiative (photon) emission. When these emissions take place close enough to the target surface, the emitted particles will be able to escape the target and be detected.

Ion bombardment induced electron emission is a frequently observed and utilized effect. Photon emission, however, has not been thoroughly studied and what results are available are inconsistent. Photon emission from a target subjected to ion bombardment was first observed by Chaudhri et al.[1–3]) who observed a continuous spectrum and attributed the emission to metal plasma oscillations. Further work by Kistemaker et al.[4,5]) and Snoek[6]) showed that the optical wavelength radiation emitted was the characteristic line spectrum of the bombarding ion and the target atom. They further concluded that the photon emission came from metastable sputtered atoms and not from atoms inside the target.

The research results reported here are those from a series of experiments which measured both photon and electron emission from targets subjected to 1 keV to 20 keV ion bombardment. The study covered the optical photon spectrum between 2000 Å and 6000 Å resulting from inelastic collisions between energetic alkali metal ions and metal and semiconductor targets. Secondary electron emission was simultaneously monitored so that comparisons could be made between

* This research was supported by a grant from the National Science Foundation.

† Present address: Centre de l'Energie, INRS, Varennes, Québec, Canada.

+ Present address: Northrop Corporation, Laser Systems Department, Hawthorne, California, U.S.A.

photon and electron emissions. These emissions were measured as functions of the experimental parameters of ion type, target material, ion energy, and current density.

2. Experimental technique

The experimental instrumentation, illustrated in fig. 1, consisted of an ion gun, a target mount goniometer and a secondary electron suppressor-collector all housed inside a vacuum chamber. Photon emission from the target was measured with a grating spectrometer which viewed the target through a sapphire window.

The vacuum chamber, a cylinder 12 inches in diameter and 15 inches tall, was of all metal construction with metal gasketed flanges, the only exception being the Viton O-ring in the sorption pump valve. All construction materials used in the vacuum were either stainless steel, aluminum, copper or ceramic so the system was bakeable to at least 200°C. The chamber was forepumped with a sorption pump to the 10^{-3} torr region and from there, the chamber was pumped by a 150 l/s ion pump to its base pressure in the mid 10^{-9} torr region. Operationally, with the ion source hot, most experiments were performed in the low 10^{-8} torr region.

Alkali metal ions were used so as to eliminate potential electron emission from the target surface. This allowed a meaningful comparison between kinetic secondary electron emission and photon emission since both emissions have their origin in inelastic collisions between the bombarding ions and the target atoms. A surface contact ionization source of the Weber and Cordes[7]) type was used. This source had a low impurity content (less than 0.1%) so that mass analysis of the beam was not necessary. The ions were accelerated, focused and collimated to a spot 10 mm^2 on the target surface. The normal operating ion gun current was 1 μA with a maximum obtainable current of 2 μA which correspond to current densities of 10 and 20 μA/cm^2, respectively. At operating pressures in the low 10^{-8} torr region these current densities insured clean target surfaces by sputtering. The beam could be diverted totally from the target without having to cool the ion source by the use of x–y deflection plates.

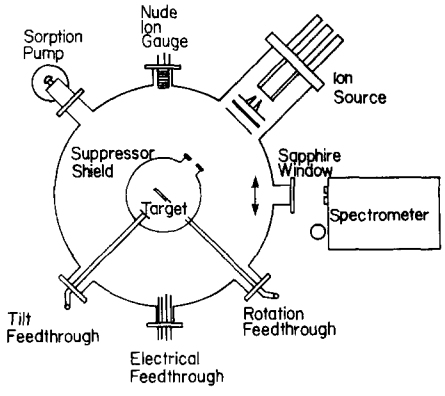

Fig. 1. Experimental configuration illustrating the 1 to 20 keV alkali metal ion source, target, secondary electron suppression shield, sapphire window and grating spectrometer.

The target was held in a fixed axis goniometer that allowed the target to be oriented in any crystallographic direction relative to the incident ion beam. The goniometer had two degrees of motion, the crystal could be rotated around an axis normal to its surface and it could also be tilted around an axis which lay in the plane of the crystal surface. These goniometer motions were controlled by bellows sealed rotary motion feedthroughs.

Two currents had to be monitored: the target ion current (I_t) and the secondary electron emission current (I_{se}). To measure the true target ion current, it was necessary to suppress the secondary electrons. This was accomplished by surrounding the target with an electrode (suppression shield) which was alternately biased at a negative potential of 100 V or grounded. At ground potential the current measured was the sum of I_t+I_{se} while with 100 V negative bias the measured current was just I_t. By this means, the secondary electron emission was obtained from the difference of the two measured quantities.

The photon emission from the target during ion bombardment passed through an aperture in the suppression shield and was focused by a quartz lens, through a sapphire high vacuum window, on to the entrance slits of the spectrometer. The spectrometer was located outside the vacuum chamber at a fixed angle of 45° relative to the ion beam. The spectrometer used was a Jarrell–Ash half meter scanning spectrometer having a range between 2000 Å and 8000 Å with a resolution of 0.2 Å. This resolution was sufficient to allow the detection of any Doppler broadening of the spectral lines.

3. Experimental results

The experimental results of interest were the spectrum of the emitted optical wavelength radiation, its intensity dependence upon the experimental parameters and the secondary electron yield.

For all combinations of bombarding ions and targets, for all energies and current densities, the only radiation emitted was the characteristic line spectrum of the ion

TABLE 1
Target and source material properties.

	Material	Z	A	λ observed (Å)
Target	Al	13	27	3961.5, 3944.0
	Si	14	28	3905.3
	Cr	24	52	4274.8
	Fe	26	56	3737.1
	Cu	29	63	3273.9, 3247.5
	Ge	32	74 (72, 70)	
	Ag	47	107 (109)	3280.6
Source	Na	11	23	5892.5
	Cs	55	133	

and target atoms. These results were consistent with those of Kistemaker et al.[4]) who also only observed line spectra, although their experimental conditions were not identical to those reported here since they used noble gas ions. The continuous spectrum reported by Chaudhri et al.[3]) for alkali metal ions bombarding metal targets is probably a result of inadequate spectral resolution in their photon detector.

Since only line spectra were observed, the results measured included the spectral shape, its intensity and the secondary electron yield. The photon detection system was not calibrated absolutely so the photon intensity results are reported in the units of photomultiplier current (nA) divided by the ion beam area (cm^2). However, since the secondary electron current was measured absolutely, the electron emission data is presented as the secondary electron yield γ, electrons per ion.

3.1. Emission spectrum and Doppler broadening

The combinations of bombarding ions and target materials investigated are tabulated in table 1, along with the characteristic line spectra observed. The spectral lines observed were the neutral atom lines indicating that the collided atoms and ions were excited to only their lowest state. For the parameters of the research, no higher excited states were observed. Within the sensitivity of the instrumentation no optical lines were observed for either cesium or germanium. The 3905 Å line of silicon was very weak, observable, but no quantitative results were obtainable.

The profile of the 3961.5 Å spectral line of aluminum bombarded by 10 keV cesium ions was measured. The ions were incident normal to the target and the photon emission was monitored at 45° from the target normal. The profile, plotted in fig. 2, had a full width at half maximum of 0.42 Å. The resolution of the spectrometer with 10 μm slits was 0.2 Å. The 3520.5 Å line of neon is plotted on the same figure to demonstrate the spectrometer resolution. As indicated by the spectral line profile there was Doppler broadening of the aluminum spectral line. The average kinetic energy of the emitting aluminum can be calculated to be 32 eV, while the average energy of an atom sputtered from a metal surface is about 50 eV. The observed Doppler broadening is consistent with this number so it is possible that the radiation comes from metastable states of sputtered particles, as proposed by Kistemaker et al.[5]).

The light emission from metastable sputtered particles does not, however, fully explain the shape of

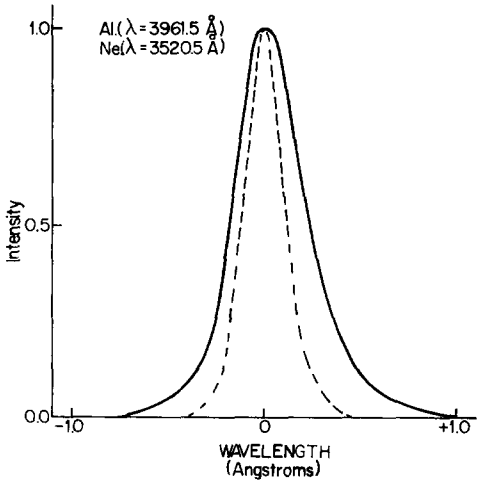

Fig. 2. Profile of the 3961.5 Å line of Al bombarded by 10 keV Cs ions and the 3520.5 Å line of Ne illustrating the spectrometer resolution.

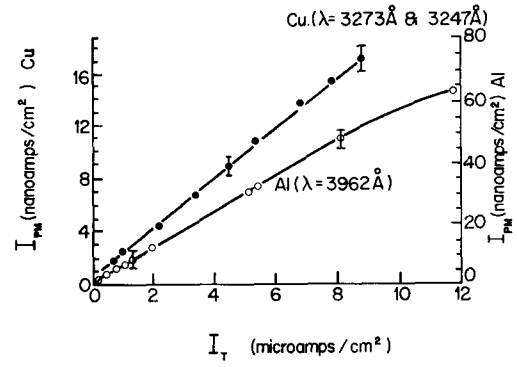

Fig. 3. Spectrometer photomultiplier current as a function of target current density for 10 keV Cs ion bombardment of Al and Cu.

the observed profile. Emission from particles moving towards the detector would cause a shift towards shorter wavelengths. The observed tail at longer wavelengths is consistent, however, with particles emitting while moving away from the spectrometer.

From fig. 2 it is clear that the bulk of the aluminum emission is unshifted and this must come from atoms which are at rest in the target lattice. In addition, the long wavelength shift indicates that excited ions are moving away from the spectrometer, or into the target, so it is concluded that photon emission comes from excited atoms inside the target besides possible sputtered metastables.

3.2. Photon and secondary electron emission dependence upon ion current density

Both the photon and secondary electron emission dependence upon current density were measured for cesium bombardment of aluminum and copper and for sodium bombardment of aluminum. For these measurements, since there was no continuous portion to the photon spectrum, the exit slips of the spectrometer were removed to increase the photomultiplier tube signal. For the copper measurements this instrumentation resulted in the two copper lines, 3273 Å and 3247 Å, being measured simultaneously.

The results for the 10 keV cesium ion bombardment of copper and aluminum are plotted in fig. 3. As can be seen, the copper photon emission intensity is linear with current density up to approximately 10 μA/cm^2. The aluminum emission is also linear up to 10 μA/cm^2, but above this current density there is a slight saturation.

The sodium-aluminum data for 10 keV sodium ions is plotted in fig. 4. Two things differ here from the cesium data. First is the presence of both sodium and aluminum emission. In the cesium bombardment case, no cesium emission was observed while in fig. 4 the sodium emission is very intense. The other significant aspect of the sodium-aluminum data is the very rapid saturation of the photon emission at approximately 2 μA/cm^2. Both the sodium and aluminum saturate at the same rate, while the secondary electron yield is still increasing linearly.

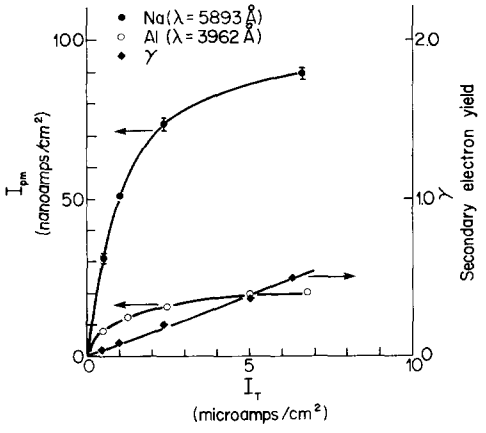

Fig. 4. Spectrometer photomultiplier current and secondary electron yield as a function of target current density for 10 keV Na ion bombardment of Al.

Saturation of the optical emission has previously been observed by Terzic and Perovic[8]) for argon bombardment on aluminum. The current density at which they observed saturation was, however, an order of magnitude above those reported here. No satisfactory explanation has been found for this behavior; the saturation of the optical spectra seems to indicate that the bombarding ions interact with the target lattice in such a way as to change the emission properties of the lattice, possibly in favor of radiationless emission.

3.3. Photon and secondary electron emission dependence upon ion energy

Photon emission and secondary electron emission were measured as a function of energy for cesium ion bombardment of the metal targets, Al, stainless steel, Cu and Ag. From stainless steel, the Fe and Cr lines were identified and the results for Fe and Cr were normalized to 100% concentration of each element. The results are given in figs. 5, 6, 7 and 8.

The photon and secondary electron emission curves are characterized by a rapid, sometimes linear, increase in intensity in the 0 to 10 keV range. At energies above this, both the photon and the secondary electron emission begin to saturate. Three competing effects influence the energy dependence of the photon emission. First, the total energy available for electron excitation increases as a result of the increase in the energy of the incident ion. The ion will deposit more energy in the crystal and hence the total amount that can be transferred to electron excitation is increased. This can be seen from the Firsov[9]) expression for the inelastic energy transfer in an ion-atom collision;

$$\xi = \frac{(Z_a + Z_b)^{5/3}\, 4.3 + 10^{-8}\, u}{[1 + 3.1\,(Z_a + Z_b)^{1/3}\, 10^7\, R_0]^5}, \qquad (1)$$

where Z_a and Z_b are the nuclear charges of the colliding particles, R_0 is the distance of closest approach and u is the incident particles speed. From this relation it can be seen that the inelastic energy loss increases with ion

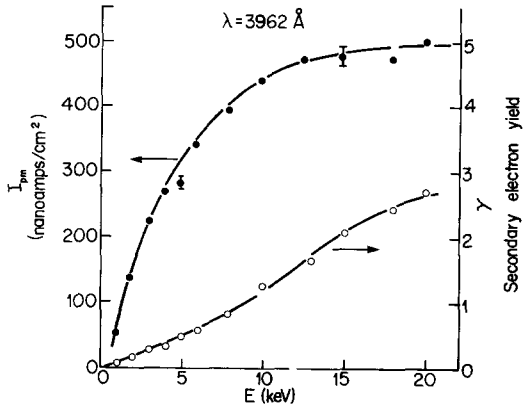

Fig. 5. Spectrometer photomultiplier current and secondary electron yield for 1 to 20 keV Cs ion bombardment of Al.

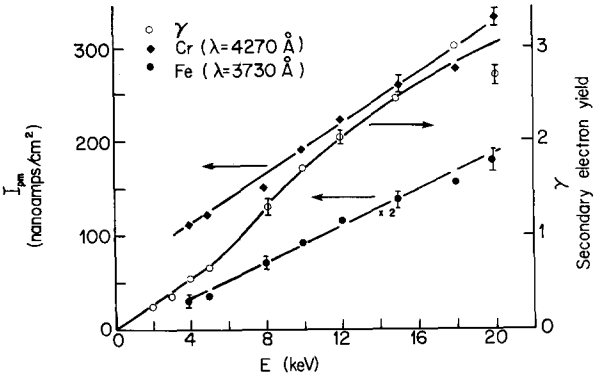

Fig. 6. Spectrometer photomultiplier current and secondary electron yield for 1 to 20 keV Cs ion bombardment of stainless steel.

energy. The measurements by Morgan and Everhart[10]) confirm the increased inelastic energy loss with increasing ion energy.

Firsov also calculated an inelastic cross section which he expressed as

$$\sigma/\sigma_0 = \left[\left(\frac{E}{E_0}\right)^{1/10} - 1\right]^2, \qquad (2)$$

where σ_0 and E_0 are constants which characterize the colliding particles. From this relation, it can be seen that the inelastic cross section increases slowly with ion energy.

The combination of the increased inelastic energy transfer and increased cross section with increasing primary ion energy accounts for the initial rapid increase in photon and secondary electron emission in the 0 to 10 keV energy range.

The third effect that will influence the photon and secondary electron emission is self-absorption by the target. As the ion energy is increased, the ions penetrate further into the target and the emitted radiations have a longer path to travel before leaving the surface. A wavelength of 3000 Å has a penetration depth (distance for the energy density to fall to 1/e of its value) of about 50 Å in aluminum[11]). This self-absorption will cause the number of observed photons to saturate as the energy of the incident ion increases.

At lower energies, for Cs ions up to 5 keV, the amount of target photon absorption is only beginning to become significant so that the inelastic energy transfer increase and the variation in cross section are the dominant effects. Consequently, the number of photons observed increases. Above 5 keV, where the ion penetration distance is comparable to or greater than the photon meanfree path (the most probable range for Cs ions in aluminum is about 250 Å at 20 keV[12] while it is 25 Å at 2 keV), the photon emission turns over and saturates with increased ion energy.

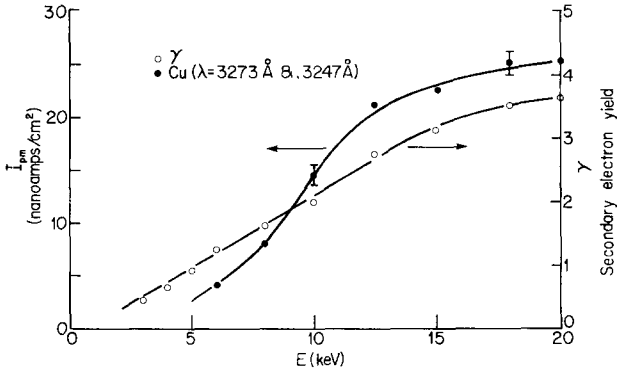

Fig. 7. Spectrometer photomultiplier current and secondary electron yield for 1 to 20 keV Cs ion bombardment of Cu.

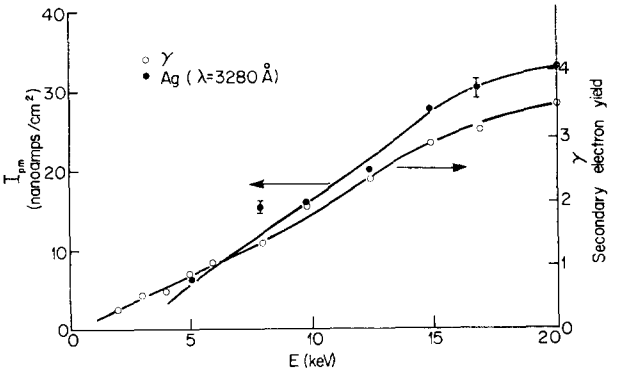

Fig. 8. Spectrometer photomultiplier current and secondary electron yield for 1 to 20 keV Cs ion bombardment of Ag.

The variation of photon emission with energy is similar but not identical to that of sputtered particles so that it is possible that the variation in emitted radiation could come from metastable sputtered particles. The major difference is that the sputtering yield reaches its maximum at lower energies, in the 5 to 10 kV range, and actually decreases above 10 keV. If photon emission originated only from sputtered metastables, the photon emission response should be similar to that of the sputtering yield.

The secondary electron yield energy dependence is similar to that of the photon production and for the same reasons. Photon and electron excitation occur in the inelastic collisions and target self-absorption diminishes the rate of increase with ion energy.

3.4. Photon and secondary electron emission dependence upon ion mass

The Firsov relation for inelastic energy transfer, eq. (1), has an approximate 5/3rd power dependence upon the sum of the ion and target atomic numbers. The denominator is little changed with Z. Although the 5/3 power dependence cannot be confirmed from the experimental data, it is clear that at a fixed energy the amount of photon and electron production is greater for the heavier ions.

Table 2

Photomultiplier current and secondary electron yield; $E = 20$ keV.

Target	Bombarding particle	Photo-multiplier current, I_{PM} (nA/cm^2)	Secondary electron yield γ	I_{PM} for Na^+ photon emission (nA/cm^2)
Cr	Na^+	47.2		
	Cs^+	305.0		
Fe	Na^+	16.0		
	Cs^+	90.0		
Al	Na^+	25.0	20.0	7.5
	Cs^+	1000.0	37.4	
Stainless steel	Na^+		22.5	12.0
	Cs^+		32.5	

The results are tabulated in table 2 for 20 keV sodium and cesium ions. For each target material investigated, the photon production and the secondary electron yield is largest, by a substantial amount, for the cesium bombardment.

4. Conclusions

The optical wavelength light emitted from targets during ion bombardment contained only line spectra characteristic of either the target and bombarding ion or both. No continuous spectrum, of the plasma oscillation type reported by Chaudhri et al.[3]), was observed.

The spectral line emission as a function of target current density was found to have an initially linear dependence at low current densities, followed by a saturation of the light output at higher current densities. The point of departure from the linear relation varied depending upon the ion–target combination. It was as low as (1 μA/cm^2) for Na^+ bombardment of Cu and above (10 μA/cm^2) for Cs^+ bombardment of Cu. No explanation is offered to explain the saturation of photon emission at the higher current densities.

The variation of photon emission with energy also exhibited a linear relation at low energy (0 to 5 keV) and then started to saturate for ion energies in the 10 keV to 20 keV range. The effect here is that as the ions penetrate deeper into the crystal there is more photon self-absorption within the target. Ion penetration distances are approximately 250 Å at 20 keV while, for metals, a photon meanfree path is approximately 50 Å.

Secondary electron emission measurements were made simultaneously with the photon measurements and in general their dependence upon the experimental parameters were similar. The saturation of photon emission with current density is unexplained, but the secondary electron emission increased linearly, as would be expected. The secondary electron emission dependence on energy was similar to that of the photon emission. The saturation of higher energies is a result of the decreased probability of electron escape. Since photon and electron emissions are produced in inelastic ion-atom collisions, the similarity of their dependence upon experimental conditions is consistent with their common origin.

References

1) R. M. Chaudhri, M. W. Kahn and A. L. Tasear, Nature **177** (1956) 1226.

2) R. M. Chaudhri and M. M. Chaudhri, Emission of ultraviolet radiation from metals under the impact of high energy positive ions, 6th Intern Conf. *Phenomena in ionized gases, II* (1963) p. 21

3) R. M. Chaudhri, M. M. Chaudhri, S. M. Kabir and M. Rafique, Angular distribution of the optical radiation emitted from Ag, Al, Cu and Ni by impact of alkali positive ions, 7th Intern Conf. *Phenomena in ionized gases, I* (1965) p. 186.

[4]) J. Kistemaker and C. Snoek, Surface phenomena related with sputtering, ion bombardment, theory and applications (CNRS, 1962) p. 71.

[5]) J. M. Fluit, L. Friedman, J. van Eck, C. Snoek and J. Kistemaker, Photon and metastable atoms produced in sputtering experiments, 5th Intern Conf. *Ionization phenomena in gases* (1961) p. 131.

[6]) C. Snoek, W. F. van der Weg and P. K. Rol, Physica **30** (1964) 341.

[7]) R. E. Weber and L. F. Cordes, Rev. Sci. Instr. **37** (1966) 112.

[8]) I. Terzic and B. Perovic, Analysis of the light emitted from the a target bombarded with high energy ions, 8th Intern. Conf. *Phenomena in ionized gases* (1967) 2.4.10.

[9]) O. B. Firsov, Soviet Phys. - JETP **36** (1959) 1075.

[10]) G. Morgan and E. Everhart, Phys. Rev. **128** (1962) 667.

[11]) M. Born and E. Wolf, *Principles of optics* (Pergamon Press, London, 1965) p. 621.

[12]) J. A. Davies, J. D. McIntyre, R. L. Cushing and M. Lounsbury, Can. J. Chem. **38** (1960) 1535.